JOURNAL OF TRAFFIC AND TRANSPORTATION ENGINEERING (ENGLISH EDITION) 2015; 2 (5): 338–345

HOSTED BY
ELSEVIER

Available online at www.sciencedirect.com
ScienceDirect
journal homepage: www.elsevier.com/locate/jtte

Original Research Paper

Safety assessment method of performance-based navigation airspace planning

Yong Tian [a,b,*], Lili Wan [b,c], Chun-hung Chen [a], Ye Yang [b]

[a] Center for Air Transportation Systems Research, George Mason University, Fairfax, VA 22030, USA
[b] School of Civil Aviation, Nanjing University of Aeronautics and Astronautics, Nanjing 210016, China
[c] National Key Laboratory of Air Traffic Flow Management, Nanjing University of Aeronautics and Astronautics, Nanjing 210016, China

ARTICLE INFO

Article history:
Available online 10 August 2015

Keywords:
Air traffic management
Safety assessment
Operational planning
Conflict risk
Adverse weather

ABSTRACT

The paper introduces a computational model of airspace conflict risk in the hierarchy of performance-based navigation (PBN) airspace operation and combines it with air traffic controller (ATC) workload to propose a method for safety assessment of PBN airspace operational planning. Capacity probability distribution is employed to depict airspace capacity in uncertain weather, errors of deviating from nominal PBN track are taken into consideration, and the stochastic process based on Gaussian distribution is used to depict random aircraft motion according to airspace PBN specification, so as to build an airspace conflict risk computational model in corresponding capacity scenario. Guangzhou No. 15 sector is chosen for simulation validation. The analysis results suggest that 60% of ATC workload is corresponding to sector traffic flow of 31 aircraft/h and airspace risk of 0.018 conflict/h, while 70% of ATC workload is corresponding to sector traffic flow of 35 aircraft/h and airspace risk of 0.03 conflict/h. As air traffic flow increases, both airspace conflict risk value and ATC workload will increase, resulting in reduction of airspace safety, though their increasing magnitudes differ with different capacity scenarios. The safety assessment method enables effective quantization of safety with regard to airspace operational planning strategy, and benefits the development of optimal operational scheme that balances risk with capacity demand.

1. Introduction

In the time of increasingly busy air transportation today, conventional navigation based airspace structure is very difficult to meet the requirement of increasing flight volume. Flight delay occurs quite often indicating a desperate need of optimization design of current airspace in China. The performance-based navigation (PBN) is a novel operational concept proposed by the International Civil Aviation Organization

* *Corresponding author*. Center for Air Transportation Systems Research, George Mason University, Fairfax, VA 22030, USA. Tel.: +86 13601589681.
E-mail address: 138139@263.net (Y. Tian).

Peer review under responsibility of Periodical Offices of Chang'an University.
http://dx.doi.org/10.1016/j.jtte.2015.08.005

(ICAO) on the basis of integrating operational practices and technical standards of country-specific area navigation (RNAV) and Required Navigation Performance (RNP), enabling effective improvements of airspace resource utilization, airspace capacity and safety. The international aviation community even regards PBN as one of the cornerstones of future air navigation system. According to China's strategy of reinvigorating the country through civil aviation, Civil Aviation Administration of China (CAAC) plans to implement PBN technology in en-route phase during the Twelfth Five-Year Plan period.

Safety is a critical issue as to whether an airspace planning scheme can be efficiently implemented or not. Safety assessment is capable of providing valid feedback information for planning, efficiently of preventing aircraft from having such hazards as conflict and collision. Therefore, airspace planning has to be built on the basis of safety assessment. Depending on different phases of air traffic management (ATM), airspace planning can be divided into strategic, tactical and operational hierarchies. Factors considered gradually increase with hierarchies and the corresponding safety assessment method varies somewhat, evaluation model has become more complicated. Safety assessment of airspace planning in various hierarchies is an important task to ensure air traffic safety.

In light of this, the scholars worldwide have conducted numerous researches. Reich (1966a, 1966b, 1966c) established the theory of aircraft collision model, firstly proposing the Reich collision risk model. Hsu (1981) put forward a concept of critical collision zone and studied aircraft collision risks on intersecting routes using conditional probability method, namely the modified Reich model. Cox et al. (1991), Harrison and Moek (1992), Moek et al. (1993) employed Reich model to study collision risks at places including North Atlantic Ocean, and analyzed probability of reducing safety separation. Brooker (2002a, 2002b) analyzed separation safety from perspective of accident analysis, studied current separation safety assessment and collision risk models, and proposed the event model (Brooker, 2003, 2004a, 2004b, 2006). Netjasov (2012a, 2012b, 2013) proposed a conflict risk evaluation model for airspace strategic planning with conflict probability and number of conflicts giving the minimum flight safety separation. Domestic studies in this field started later, Zhao (1998) studied number of dangerous conflicts occurring on aircraft at two intersecting air routes. Ying and Xu (2002) and Xu et al. (2008) employed Reich model to study the issue of safety assessment of separation criterion at parallel routes in oceanic area and built the event model based on collision cylinder. Han et al. (2006) improved the collision risk model under the condition of radar separation and proposed a computational model at radar control separation where it is necessary for air traffic controller to intervene any flight conflict with or without non-intrusion zone. The researches on airspace safety assessment worldwide primarily started from collision risk, focusing on collision risk model and safety separation determination, but there were only fewer studies focusing on conflict risk. Moreover, they mainly used two routes, not applying their researches to all airspace planning cases, such as ad-hoc sectorization (Zhang et al., 2007, 2009; Meng et al., 2010; Zhou et al., 2014).

In this paper, weather uncertainty factor and error of aircraft flight deviating from PBN nominal track are taken into account for airspace planning operational hierarchy. Actual track is simulated using stochastic method based on Gaussian distribution, thereby random airspace conflict risk in corresponding capacity scenario is studied. With ATC workload as an indicator to represent human factor impact, a method for safety assessment of PBN airspace operational planning is proposed, thereby different airspace design and organizational scenarios are compared and validated through computation of test cases.

2. Problem description

During actual aircraft operations, flight safety will be subject to such factors as complexity of air route structure and features of traffic flow in airspace. While the PBN specification is selected, weather change and human factor would further increase uncertainty of flight safety. If PBN specifications selected varies, then errors of deviating from nominal track would differ somewhat; occurrence of adverse weather would aggravate the difficulty of pilot operation, directly impairing the flight safety. Meanwhile, weather change leads to uncertainty of airspace capacity. Once airspace capacity decreases, congestion phenomenon would appear, resulting in increased ATC workload. If the load exceeds affordable ATC load limit, the response rate and air control efficiency of an air traffic controller would decrease dramatically, and it would be too late to control some aircraft in "potentially dangerous conflict state", resulting in potential safety hazard.

What has bean considered in this paper is the safety assessment method in airspace operational planning hierarchy, such assessment usually lasts a week, so information about aircraft type and traffic flow in airspace is certain. This model mainly combines airspace conflict risk and ATC workload to compare various operational scenarios of airspace, so as to balance airspace conflict risk and traffic flow demand, which are beneficial to developing a flight plan with low risk and high traffic flow and to enabling air traffic flow assignment in case of uncertain weather. The model can be used in PBN airspace operational planning stages, such as discriminating the responsibilities of an air traffic controller from those of a pilot, ad-hoc adjustment of flight plan and dynamic sectorization. To simplify the model, the following assumptions are adopted.

(1) When an aircraft flies in a PBN airspace, its error of deviating from nominal track follows Gaussian distribution.
(2) Conflict risk value is not a constant, but is related to airspace structure and weather information, etc.
(3) Influences of on-board devices and others on conflict risk are disregarded.

3. Safety assessment model

The model proposed in this paper makes safety assessment from macroscopic perspective. With the combination of airspace conflict risk and ATC workload as an assessment indicator, the safety assessment model can be used to aid in selection of decision strategy in airspace operational planning stage, reduce airspace risk and to balance traffic flow. The model framework is shown in Fig. 1. Conflict risks mainly depend on the airspace structure, adopted PBN specification, safety separation setting and weather change, among which weather change and PBN derived navigation error are the most important factors of airspace operational uncertainty. Therefore, it is necessary to take control of weather-derived capacity change and simulate yaw error, so as to study airspace risk and ATC workload in case of capacity uncertainty, which is an effective support tool for expert operational decision.

3.1. *Capacity probability distribution curve*

Usually, a capacity probability distribution curve can express the relationship between capacity and its corresponding probability (Clarke et al., 2013). This paper utilizes the capacity probability distribution curve to calculate the average airspace capacity of every weather scenario, build mapping of airspace average capacity versus weather scenario, and to obtain the average capacity probability distribution curve. With PBN navigation error, airspace traffic flow in the weather scenario is simulated to generate actual track and detect the conflict, and then to obtain airspace conflict risk value in case of uncertain weather.

In the entire safety assessment model, the average capacity probability distribution curve is mainly used to depict airspace capacity uncertainty, enable real and vivid reflection of weather impact on airspace capacity, and facilitate analysis of conflict risk in uncertain airspace. As illustrated in Fig. 2, owing to the uncertainty of weather change, a certain probability of occurrence exists in each type of weather scenario for the corresponding airspace capacity. In regard to airspace capacity probability distribution curve, its building process mainly consists of weather scenario generation and random capacity determination. The capacity distribution is obtained through analysis of history data using *K*-means clustering or through computer simulation.

By analyzing the capacity probability distribution curve each type of weather scenarios, the average airspace capacity in a certain weather scenario $\overline{R}$ is calculated as follow

$$\overline{R} = \int RPdt \tag{1}$$

where P denotes the probability of capacity in certain weather scenario, R is the average capacity. There are several kinds of weather scenarios in each time slice. There is a certain probability for each weather scenario, hence a correspondence of weather scenario probability and airspace average capacity can be created. As illustrated in Fig. 3, probability of weather scenario A occurrence is P_1, while the airspace average capacity is R_1. That is to say, the probability of capacity R_1 occurrence is P_1 (airspace average capacity varies with weather scenario), and the sum of all capacity scenarios probabilities is 1.

3.2. *Assessment of PBN airspace conflict risk*

In airspace operational planning stage, the flight plan is known. When weather change makes capacity decrease so as

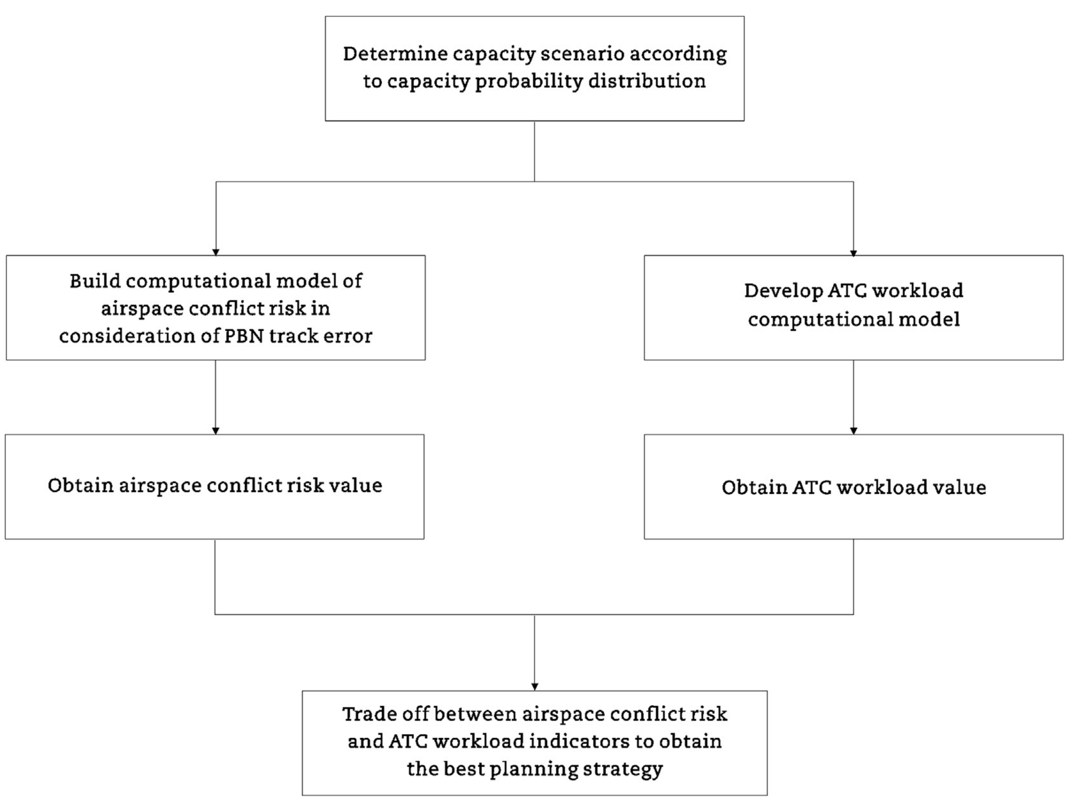

Fig. 1 – Schematic of safety assessment model framework.

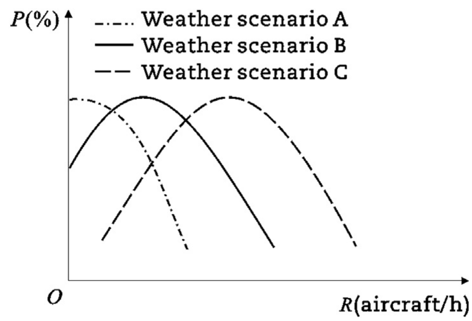

Fig. 2 – Schematic of capacity probability distribution curve.

not to match the air traffic flow, traffic flow has to be reassigned according to capacity constraint. Throughout the process of computing airspace conflict risk, the traffic flow is firstly simulated in a fixed airspace with consideration of PBN navigation specification, so as to generate actual track deviating from nominal track, and the number of aircraft conflicts in this run of simulation is calculated using conflict detection method, which is then combined with weather scenario occurrence probability to obtain airspace conflict risk value in this capacity scenario.

3.2.1. *Prediction of actual track*

Actual track of aircraft flying is often subject to uncertain factors such as PBN navigation specification used, crosswind, etc., thus actual track often deviates from nominal track and follows a certain rule. In this paper, influences of PBN navigation on actual track are taken into account. The formula of actual track is shown as follow

$$d\overrightarrow{X_t} = \overrightarrow{v_t}dt + \overrightarrow{\sigma_t}dt \tag{2}$$

where $\overrightarrow{X_t}$ denotes the position of aircraft at time t, $\overrightarrow{v_t}$ denotes the speed of aircraft at time t, $\overrightarrow{\sigma_t}$ denotes the error of aircraft at time t. All the above parameters are three-dimensional vectors.

The PBN type for en-route operation is established according to navigation performance accuracies in horizontal plane (i.e., lateral and longitudinal navigation accuracies), and its performance parameters include accuracy, availability, continuity and integrity. Among the performance parameters, accuracy is an immediate factor causing yaw of aircraft

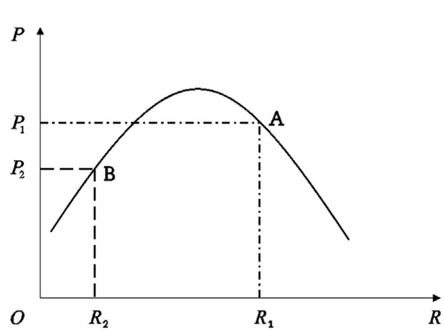

Fig. 3 – Average capacity probability distribution curve.

position. Since PBN usually depicts airspace properties via navigation accuracy, the PBN accuracy derived aircraft yaw error is primarily considered in this paper.

As defined, PBN mainly consists of two specifications, RNAV and RNP. Accuracies of RNAV and RNP specifications can be expressed as accuracy values guaranteeing that an aircraft is capable of achieving expected navigation performance on an airspace or route within 95% of airspace flight period. The total navigation system error in any single flight must not exceed the specified RNP type for 95% of the flight time on any portion of the flight. In the event that flight procedure navigation specifications are RNAV-*n* and RNP-*n*. Since the horizontal trajectory error follows Gaussian distribution, it can be known that total systematic errors of longitudinal and lateral navigations are

$$\epsilon_n^x \sim N\left(0, \left(\frac{n}{1.96}\right)^2\right), \ \epsilon_n^y \sim N\left(0, \left(\frac{n}{1.96}\right)^2\right) \tag{3}$$

As to the vertical error of an aircraft flying as per PBN procedure, it is not stipulated in ICAO and PBN manuals. Here it can be assumed to conform to general empirical vertical navigation error ϵ_n^z. Thereby aircraft position at time t can be determined as follow

$$\overrightarrow{X_t} = \int_0^t \overrightarrow{v_t}dt + \int_0^t \overrightarrow{\sigma_t}dt = \int_0^t \overrightarrow{v_t}dt + \left(\epsilon_n^x, \epsilon_n^y, \epsilon_n^z\right)^T \tag{4}$$

3.2.2. *Conflict detection*

In the case of aircraft en-route flight, conflicts consist of the conflict between aircraft and adverse weather and the conflict between aircrafts from perspective of conflict object and from perspective of space. Conflicts mainly include horizontal conflict and vertical conflict. The vertical conflict can be identified with vertical separation, whereas horizontal conflict is more complex and will be predominantly discussed below. The conflict between aircraft and adverse weather is mainly controlled by separation limits, where information of adverse weather can be obtained from CAAC weather forecast and radar reflection. When an aircraft is flying in adverse weather, the space for turn and withdrawal must be taken into account. To reduce the impact of adverse weather on aircraft, a concept of flight-restricted zone is developed. In consideration of adverse weather information and compliance with current regulation allowing aircraft to fly around in China, flight-restricted zone is obtained, which is an irregular geometric shape from perspective of horizontal plane, as shown in Fig. 4.

An aircraft in adverse weather needs to meet certain safety separation in space, that is, the aircraft is refrained from admitting into the irregular-shaped flight-restricted zone due to adverse weather, as shown in Fig. 5. The radius of the safety zone is a larger size between the aircraft fuselage and wingspan.

As trajectory of aircraft i extends at speed $\overrightarrow{v}_i$ to cross the flight-restricted zone, aircraft i would conflict with adverse weather and has to fly around. Every aircraft has a circular safety zone, which has to be beyond the flight-restricted zone. The slopes of tangent lines between the aircraft safety zone and flight-restricted zone relative to their intersecting line are

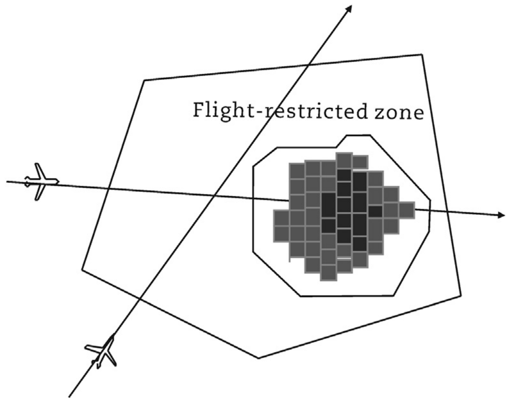

Fig. 4 – Schematic of flight-restricted zone position.

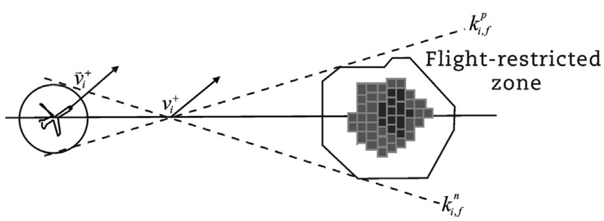

Fig. 5 – Weather safety separation.

$k_{i,f}^p$ and $k_{i,f}^n$, respectively. To guarantee flight safety, aircraft i and the flight-restricted zone have to satisfy the following conditions.

$$\vec{v}_{i,y} \geq \vec{v}_{i,x} k_{i,f}^p,\ \vec{v}_{i,x} \geq 0 \tag{5}$$

$$\text{or}\quad \vec{v}_{i,y} \leq \vec{v}_{i,x} k_{i,f}^n,\ \vec{v}_{i,x} \geq 0 \tag{6}$$

$$\text{or}\quad \vec{v}_{i,x} \leq 0 \tag{7}$$

The trajectories between aircrafts have to meet separation limit too, similar to the case of adverse weather, as shown in Fig. 6. Every aircraft safety zone is a circular area, and aircraft i and j have to satisfy the following condition.

$$\vec{v}_{i,j,y} \geq \vec{v}_{i,j,x} k_{i,j}^p,\ \vec{v}_{i,j,x} \geq 0 \tag{8}$$

$$\text{or}\quad \vec{v}_{i,j,y} \leq \vec{v}_{i,j,x} k_{i,j}^n,\ \vec{v}_{i,j,x} \geq 0 \tag{9}$$

$$\text{or}\quad \vec{v}_{i,j,x} \leq 0 \tag{10}$$

3.2.3. *Calculation of conflict risk*

There exists a certain probability in forecast of future weather due to weather uncertainty. In this paper, update cycle of weather information is t, weather capacity scenarios obtained in various update cycles are denoted as set $M = \{1, \cdots, m\}$, of which element m contains three variables, $m = (A_m, P_m, R_m)$, where A_m denotes weather type, P_m denotes probability of weather scenario A_m occurring, R_m denotes corresponding airspace capacity of weather scenario A_m. By means of Monte Carlo simulation, number N_m of conflicts can be obtained in case of weather scenario A_m, where N_m is a discrete variable expressed as follow

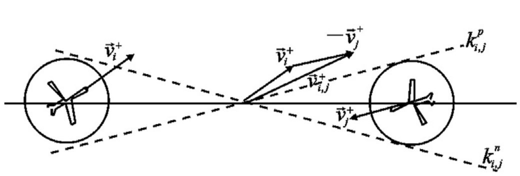

Fig. 6 – Aircraft safety zone.

$$N_m \sim \begin{pmatrix} 0 & N_1 & N_2 & \cdots & N_m \\ 0 & P_1 & P_2 & \cdots & P_m \end{pmatrix} \tag{11}$$

$$\sum_{k=0}^{m} P_k = 1,\ R_m \sim \begin{pmatrix} 0 & R_1 & R_2 & \cdots & R_m \\ 0 & P_1 & P_2 & \cdots & P_m \end{pmatrix}$$

In order to assess severity of airspace conflict risk, this paper defines that conflict risk value C is the number of conflicts probably occurring per hour. Unlike collision risk value, which evaluates the collision risk, conflict risk value mainly evaluates the conflict risk.

$$c_i = N_i P_i \tag{12}$$

$$C = \sum_{i=1}^{m} c_i = \sum_{i=1}^{m} N_i P_i \tag{13}$$

where c_i denotes corresponding airspace conflict risk value in weather scenario A_i, C denotes total conflict risk value in airspace at time t.

3.3. *Assessment of ATC workload*

During assessment, human factor is extremely important. The human factor in this paper is embodied by ATC workload. As airspace traffic flow rises, both the number of conflicts and ATC workload increase. But their growth trends are different. To balance traffic flow and airspace safety risks, experts can make decisions according to the relationship among conflict risk value, traffic flow, and ATC workload, and choose the appropriate traffic flow and acceptable degree of airspace safety risk.

The job of air traffic controllers is mainly divided into three types, communication, non-communication and thinking. The communication-type job includes receiving aircraft, adjusting aircraft altitude and speed, radar vectoring aircraft, and offering meteorological intelligence. The non-communication-type job includes monitoring aircraft, seeking flight progress strip, and filling in flight progress strip. The thinking-type job includes computing aviation elements and developing preliminary conflict solution. Since ATC workload in this paper is obtained on the basis of simulation, conflict might be present. In order to highlight the impact of conflict on load, ATC workload is computed at two stages. One is to compute basic air control load, which is the workload unavoidable under the condition of certain airspace structure and air control rule, however, conflict situation in airspace changes, which is a linear relationship with traffic flow in the airspace. The other is to reallocate computation of air control load, which is the workload resulting from resolving flight conflict among aircraft, given certain airspace structure and air control condition.

Total sector workload within time slice t is expressed as follow

$$W(t) = \sum_{j=0}^{s} W_j(t) = \sum_{j=0}^{s} \left(W_j^{st}(t) + W_j^{dy}(t) \right) \tag{14}$$

where $W(t)$ denotes total ATC workload within time slice t, $W_j(t)$ denotes total ATC workload on route j within time slice t, $W_j^{st}(t)$ denotes basic air control load on route j within time slice t, $W_j^{dy}(t)$ denotes reallocated air control load on route j within time slice t.

Depending on the reallocation method at conflict onset, reallocation of air control load can be generally divided into three types, altitude reallocation, speed reallocation and direction reallocation (Wan and Hu, 2006), corresponding to different reallocated air control loads respectively, the calculation formula is shown as follow

$$W_{sjt}^{dy}(t) = t_h \tau_{hj} + t_v \tau_{vj} + t_d \tau_{dj} \tag{15}$$

where t_h denotes weight of altitude-reallocation-type air control load, t_v denotes weight of speed-reallocation-type air control load, t_d denotes weight of direction-reallocation-type air control load, τ_{hj} denotes number of altitude reallocation operations in air control on route j within time slice t, τ_{vj} denotes number of speed reallocation operations in air control on route j within time slice t, τ_{dj} denotes number of direction reallocation operations in air control on route j within time slice t.

4. Analysis of computational example

Guangzhou No. 15 sector in central south China region is a typical busy flight sector in China, where there are many route intersecting points and a lot of potential conflicts. In this paper, this sector model is chosen for simulation validation.

This sector is often subject to weather conditions. In particular, occurrence of bumpy weather would result in many flight levels unavailable. One day in 2013, SIGMET message was received predicting bumpy weather. Based on message information and radar detection, the flight-restricted zone position is illustrated in Fig. 7. This study covers time range from UTC 0900 to UTC 1000, take 1 h as one time slice, in which there are 5 capacity scenarios. Capacity probability distribution could be obtained using the reference method due to weather uncertainty (Clarke et al., 2013), expressed as follow

$$R_m \sim \begin{pmatrix} 0 & R_1 & R_2 & \cdots & R_m \\ 0 & P_1 & P_2 & \cdots & P_m \end{pmatrix} \sim \begin{pmatrix} 0 & 10 & 20 & 30 & 40 & 50 \\ 0 & 0.01 & 0.03 & 0.54 & 0.35 & 0.07 \end{pmatrix}$$

The en-route aircraft in the sector are primarily of type C, with a speed of 720 km/h. The PBN specification adopted by the routes is RNAV 2, while traffic flow distribution of each route is shown in Table 1.

From analysis of route structure and air traffic flow distribution, it is known that the conflicts are mainly converging conflicts occurring at LKO and HZ. In air traffic control, the empirical value of ATC safety separation is 15 km or 20 km, which in this paper will be set at 10, 15 and 20 km, respectively, to facilitate model comparison and validation. When aircraft safety separation is 10 km, the number of conflicts corresponding to capacity is obtained through Monte Carlo simulation. Conflict probability distribution is expressed as follow

$$N_m \sim \begin{pmatrix} 0 & N_1 & N_2 & \cdots & N_m \\ 0 & P_1 & P_2 & \cdots & P_m \end{pmatrix} \sim \begin{pmatrix} 0 & 0.0048 & 0.0053 & 0.0184 & 0.0460 & 0.0508 \\ 0 & 0.01 & 0.03 & 0.54 & 0.35 & 0.07 \end{pmatrix}$$

Calculation using Eqs. (12) and (13) yields the total sector conflict risk value, 0.03 times/h. In the simulation, route structure derived conflict impact is mainly considered, hence rear-ended conflict is disregarded. Now capacity scenarios 1, 2, 3 and 4 are selected for analysis and their corresponding sector capacities are 10, 20, 30 and 40 aircraft/h, so that conflict risk values and ATC workload values at various safety separations and various capacity scenarios can be obtained, as shown in Fig. 8. As airspace traffic flow rises, the number of conflicts and ATC workload increase accordingly. Meanwhile,

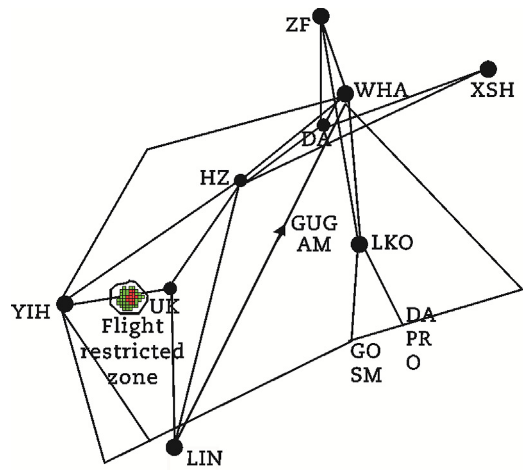

Fig. 7 – Geometric distribution of sector routes in adverse weather.

Table 1 – Distribution of en-route traffic flow.

Name of route	Ratio of air traffic flow (%)	Name of route	Ratio of air traffic flow (%)
ZF-LKO-GOSMA	5.9	YIH-HZ-WHA	9.3
GOSMA-LKO-ZF	6.6	DA-HZ-LIN	1.4
ZF-LKO-DAPRO	26.9	LIN-HZ-DA	1.8
DAPRO-LKO-ZF	24.9	WHA-LIN	2.5
WHA-HZ-YIH	8.1	LIN-WHA	1.4
DA-HZ-YIH	1.6	XSH-DA-LKO-GOSMA	0.9
GOSMA-LKO-WHA	1.1	YIH-HZ-XSH	1.1
DAPRO-LKO-WHA	1.3	LKO-DAPRO	2.5
DAPRO-LKO	1.8	WHA-LKO-GOSMA	0.9

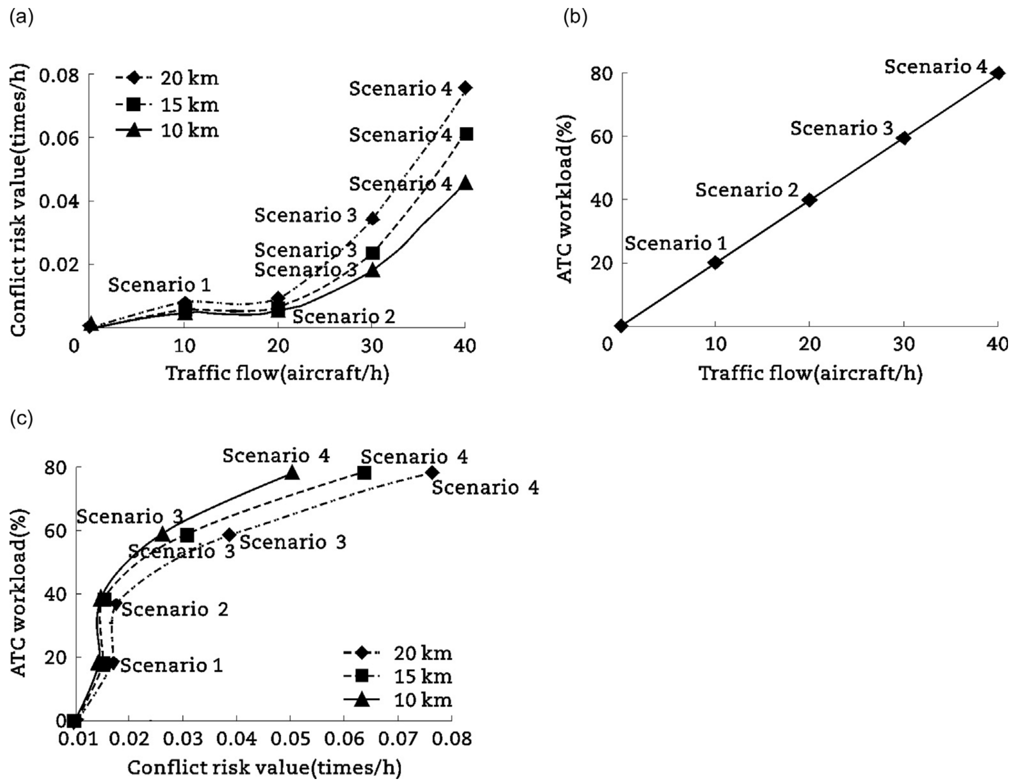

Fig. 8 – Relationship among traffic flow, conflict risk value and ATC workload. (a) Curves of traffic flow versus conflict risk value. (b) Curve of traffic flow versus ATC workload. (c) Curves of conflict risk value versus ATC workload.

the greater the safety separation setting value, the bigger the number of conflicts. The less the conflicts, the less the deployment of control load. So the basic control load is as the main part which is a linear relationship with the traffic flow. Increased number of conflicts and ATC workload will result in increased airspace safety risk. To balance traffic flow and airspace safety risks, experts can make decisions according to the relationship among conflict risk value, traffic flow, and ATC workload, and choose appropriate traffic flow and acceptable degree of airspace safety risk. As shown in Fig. 8, 60% of ATC workload correspond to sector traffic flow of 31 aircraft/h and airspace risk of 0.018 conflict/h, while 70% of ATC workload correspond to sector traffic flow of 35 aircraft/h and airspace risk of 0.03 conflict/h. At present, ICAO has no quantitative indicator with regard to conflict risk, by referring to CAAC Air Traffic Safety Assessment & Management Methods and risk probability classification table in ICAO Doc 9859 Safety Management Manual. It is known that when airspace conflict risk is no less than 1×10^{-3}/h, the risk level is level 1, conflicts are frequent; when both schemes are compared, if ATC workload and airspace risk are expected low, the former scheme can be chosen; if airspace operational efficiency is expected to increase, the latter scheme can be chosen; choice of strategy relates with how individual expert accepts safety and traffic flow. Furthermore, to mitigate impact of ATC workload, experts can take such measurement as reallocate responsibilities of air traffic controller and pilot or implementing dynamic sectorization strategy, which can balance the sector control load and reduce the risk of high load sectors airspace.

5. Conclusions

This paper proposes a safety assessment model for PBN airspace operational planning. This model takes the weather uncertainty factor into account, identifies capacity scenarios with the capacity probability distribution, and studies conflict risks in various capacity scenarios. In the consideration of the error of aircraft deviating from nominal track when flying along the nominal track in every PBN flight procedure, the stochastic process based on Gaussian distribution is employed to depict random aircraft motion derived from PBN specification, meanwhile ATC workload is served as an indicator in view of human factor, airspace safety is further assessed, and finally this method is validated with is test case. The computational results suggest that, the greater the airspace conflict risk value, the higher the ATC workload, and the worse the airspace safety. In the operational planning, flight safety can be improved by adopting strategies such as changing safety separation, reducing air traffic flow and dynamic sectorization.

The model proposed in this paper mainly assesses airspace safety in view of providing decision support for PBN airspace planning. It can be used to aid developing a rational airspace operational scheme to balance the conflict risk and flight demand, and further to provide a theoretical basis for future PBN airspace planning based on the safety assessment.

Acknowledgments

This study is supported by the Fundamental Research Funds for the Central Universities (NJ20140017).

REFERENCES

Brooker, P., 2002a. Future air traffic management: quantitative en route safety assessment, part 1-review of present methods. Journal of Navigation 55 (2), 197–211.
Brooker, P., 2002b. Future air traffic management: quantitative en route safety assessment, part 2-new approaches. Journal of Navigation 55 (3), 363–379.
Brooker, P., 2003. Lateral collision risk in air traffic track systems: a 'post-Reich' event model. Journal of Navigation 56 (3), 399–409.
Brooker, P., 2004a. Radar inaccuracies and mid-air collision risk: part 1 a dynamic methodology. Journal of Navigation 57 (1), 25–37.
Brooker, P., 2004b. Radar inaccuracies and mid-air collision risk: part 2 en route radar separation minima. Journal of Navigation 57 (1), 37–51.
Brooker, P., 2006. Longitudinal collision risk for ATC track systems: a hazardous event model. Journal of Navigation 59 (1), 55–70.
Clarke, J.P.B., Solak, S., Ren, L.L., et al., 2013. Determining stochastic airspace capacity for air traffic flow management. Transportation Science 47 (4), 542–559.
Cox, M.E., Ten Have, J.M., Forrester, D.A., 1991. European studies to investigate the feasibility of using 1000 ft vertical separation minima above FL 290, parts I. Journal of Navigation 44 (2), 171–183.
Han, S.C., Pei, C.G., Sui, D., et al., 2006. Security analysis of area navigation parallel airway. Acta Aeronautica et Astronautica Sinica 27 (6), 1023–1027.
Harrison, D., Moek, G., 1992. European studies to investigate the feasibility of using 1000 ft vertical separation minima above FL 290, parts II. Journal of Navigation 45 (1), 91–106.
Hsu, D.A., 1981. The evaluation of aircraft collision probabilities at intersecting air routes. Journal of Navigation 34 (1), 78–102.
Meng, X.W., Zhang, P., Wang, Y., 2010. Aircraft collision risk assessment at intersecting air routes. Journal of Beijing University of Aeronautics and Astronautics 36 (9), 1021–1025.
Moek, G., Ten Have, J.M., Harrison, D., et al., 1993. European studies to investigate the feasibility of using 1000 ft vertical separation minima above FL 290, parts III. Journal of Navigation 46 (2), 245–261.
Netjasov, F., 2012a. Framework for airspace planning and design based on conflict risk assessment part 1: conflict risk assessment model for airspace strategic planning. Transportation Research Part C: Emerging Technologies 24, 190–212.
Netjasov, F., 2012b. Framework for airspace planning and design based on conflict risk assessment part 2: conflict risk assessment model for airspace tactical planning. Transportation Research Part C: Emerging Technologies 24, 213–226.
Netjasov, F., 2013. Framework for airspace planning and design based on conflict risk assessment part 3: conflict risk assessment model for airspace operational and current day planning. Transportation Research Part C: Emerging Technologies 32, 31–47.
Reich, P.G., 1966a. Analysis of long-range air traffic systems: separation standards I. Journal of Navigation 19 (1), 88–98.
Reich, P.G., 1966b. Analysis of long-range air traffic systems: separation standards II. Journal of Navigation 19 (2), 169–186.
Reich, P.G., 1966c. Analysis of long-range air traffic systems: separation standards III. Journal of Navigation 19 (3), 331–347.
Wan, L.L., Hu, M.H., 2006. Research on the evaluation of controller's workload and the sector capacity. Journal of Transportation Engineering and Information 4 (2), 70–75.
Xu, X.H., Wang, Z.Y., Zhao, H.S., 2008. Improved lateral collision risk model based on event. Journal of Civil Aviation University of China 26 (3), 1–4.
Ying, A.L., Xu, X.H., 2002. REICH model in collision risk study of airspace flight. Journal of Civil Aviation University of China 20 (4), 6–10.
Zhang, Z.N., Zhang, X.Y., Li, D.B., 2007. Computation model of lateral collision rate on parallel routes based on VOR navigation. Journal of Traffic and Transportation Engineering 7 (3), 21–24.
Zhang, Z.N., Liu, J.M., Wang, L.L., 2009. Assessment of longitudinal collision risk on parallel routes based on communication, navigation, and surveillance performances. Journal of Southwest Jiaotong University 44 (6), 918–925.
Zhao, H.Y., 1998. Study on the model for computing the number of dangerous conflicts among aircrafts on two intersecting tracks. Journal of Systems Engineering and Electronics 20 (5), 6–8. 17.
Zhou, J., Zhou, Q., Jiang, Z.W., 2014. Study on safety assessment of parallel route based on lateral separation model. China Safety Science Journal 24 (8), 26–30.